Assessing Hydrated Cement Paste Properties Using Experimentally Informed Discrete Models

Šavija, Branko; Zhang, Hongzhi; Schlangen, E.

DOI
10.1061/(ASCE)MT.1943-5533.0002772

Publication date
2019

Document Version
Final published version

Published in
Journal of Materials in Civil Engineering

Citation (APA)
Šavija, B., Zhang, H., & Schlangen, E. (2019). Assessing Hydrated Cement Paste Properties Using Experimentally Informed Discrete Models. *Journal of Materials in Civil Engineering*, *31*(9), Article 04019169. https://doi.org/10.1061/(ASCE)MT.1943-5533.0002772

Assessing Hydrated Cement Paste Properties Using Experimentally Informed Discrete Models

Branko Šavija[1]; Hongzhi Zhang[2]; and Erik Schlangen[3]

Abstract: Properties of concrete are, to a large extent, dependent on the properties of its binding constituent, hydrated cement paste. Therefore, knowledge of properties of hydrated cement paste is crucial for predicting concrete behavior. This paper presents an experimentally informed approach for modeling elastic and transport properties of cement paste. The models used realistic microstructural information—obtained by X-ray computed tomography—as input for property determination. The properties were then determined using discrete numerical models, namely, models based on a lattice approach. Modeling results were compared with literature data, showing excellent correlations. Furthermore, dependence of properties of cement paste on the total porosity, based on the modeling results, was explored. Finally, a correlation between elastic and transport properties for the explored range of portland cement pastes was established. It is seen that the models can be used for property prediction, but also for exploring correlations between different parameters. **DOI: 10.1061/(ASCE)MT.1943-5533.0002772.**

Author keywords: Cement paste; Young's modulus; Chloride diffusion; Lattice model; X-ray computed tomography.

Introduction

Properties of concrete are, to a great extent, determined by the properties of its main constituent: cement paste (Powers and Brownyard 1946). This is valid for the mechanical properties, such as strength (Toutanji and El-Korchi 1995) and elastic modulus (Hirsch 1962), but also for the durability, measured through, e.g., transport properties such as permeability (Ye 2003). Simulation and prediction of property development in cement pastes is therefore a major topic of research in the field of cementitious materials.

In the past decade or so, numerous approaches for simulating property development of cement paste have been proposed. In general, these approaches comprise two parts: simulation of hydration and microstructure development, and simulation of the property (e.g., elastic modulus, strength, or diffusivity) itself. Therefore, a good description of the microstructure is the first step. A number of computer models for microstructure development have been presented. In most models, cement particles are simulated as spherical (Bishnoi and Scrivener 2009; Ye 2003), which has a certain influence on the resulting microstructural properties such as porosity and pore connectivity. Models that consider realistic particle shapes provide an improved description of the morphology (Bentz 2006; Liu et al. 2018). An additional possibility is to use a real microstructure—obtained by, e.g., scanning electron microscopy in two dimensions (2D) (Çopuroğlu and Schlangen 2008; Luković et al. 2014) or X-ray computed tomography (CT) in three dimensions (3D) (Gallucci et al. 2007)—as a basis for determining the properties of the material. Compared to computer-generated microstructures, these approaches provide a more realistic description of the microstructure. However, this is limited by the spatial resolution of the acquired image. Despite this drawback, this approach was used in this research. Since microstructures obtained experimentally (as opposed to simulated microstructures) are directly used as input for numerical simulations, this approach is considered to be experimentally informed. Since commonly used microstructural models can only describe the real microstructure in a simplified way, this paper proposes an approach that avoids this issue by using experimental microstructural data as input.

The next step is the use of a (numerical) model to determine the effective properties of the material based on its microstructure. Models based on micromechanics are commonly used (Damrongwiriyanupap et al. 2017; Haecker et al. 2005; Pichler et al. 2009). Numerical approaches like finite-element models (Montero-Chacón et al. 2014) or lattice-type models (Sherzer et al. 2017) are also widespread. While each of these approaches has advantages and drawbacks, all are dependent on the microstructural input for providing reliable results. In this research, experimentally obtained microstructures were directly used as input for simulating transport (diffusivity) and mechanical (elastic modulus) properties of cement pastes of various ages. Simulation results were first validated by comparing them to experimental observations. Then properties of cement pastes for different water-to-cement (w:c) ratios and ages were determined. This work had two aims: first, it tried to establish the experimentally informed modeling procedure as a viable option for obtaining properties of multiphase porous materials such as cement paste; and second, it explored relationships between mechanical and transport properties (chloride diffusivity) of cement paste.

[1]Assistant Professor, Microlab, Faculty of Civil Engineering and Geosciences, Delft Univ. of Technology, Stevinweg 1, 2628 CN Delft, Netherlands. ORCID: https://orcid.org/0000-0003-1299-1449. Email: b.savija@tudelft.nl

[2]Ph.D. Candidate, Microlab, Faculty of Civil Engineering and Geosciences, Delft Univ. of Technology, Stevinweg 1, 2628 CN Delft, Netherlands (corresponding author). ORCID: https://orcid.org/0000-0002-7474-4665. Email: h.zhang-5@tudelft.nl

[3]Professor, Microlab, Faculty of Civil Engineering and Geosciences, Delft Univ. of Technology, Stevinweg 1, 2628 CN Delft, Netherlands. ORCID: https://orcid.org/0000-0001-5671-8888. Email: erik.schlangen@tudelft.nl

Note. This manuscript was submitted on July 5, 2018; approved on January 30, 2019; published online on June 17, 2019. Discussion period open until November 17, 2019; separate discussions must be submitted for individual papers. This paper is part of the ***Journal of Materials in Civil Engineering***, © ASCE, ISSN 0899-1561.

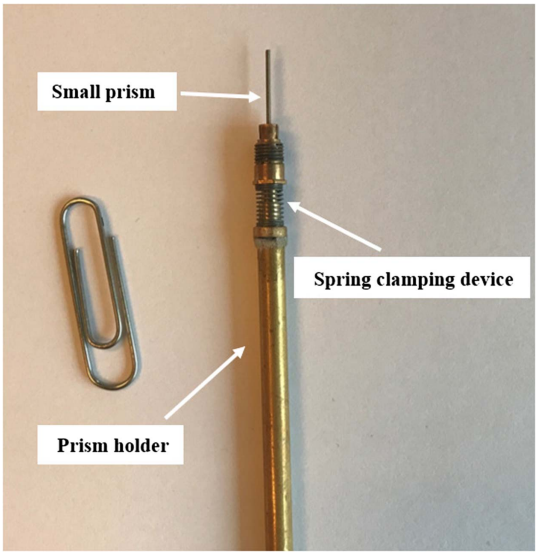

Fig. 1. Microbeam specimen clamped on the holder prior to X-ray computed tomography experiment. (Reprinted from *Cement and Concrete Research*, Vol. 102, H. Zhang, B. Šavija, S. Chaves Figueiredo, and E. Schlangen, "Experimentally validated multi-scale modelling scheme of deformation and fracture of cement paste," pp. 175–186, © 2017, with permission from Elsevier.)

Experiments

Materials

Specimens of cement paste with three w:c ratios (0.3, 0.4, and 0.5) were prepared by mixing ordinary portland cement (CEM I 42.5 N, ENCI, Maastricht, Netherlands) and demineralized water. After mixing, pastes were cast in plastic cylinders with 24-mm diameter and 39-mm height. Fresh mixtures were compacted on a vibrating table to remove air bubbles. In order to prevent bleeding, sealed cylinders were rotated slowly (2.5 rpm) for 24 h. Afterward, the specimens were cured under sealed conditions in a laboratory environment (approximately 20°C) until reaching testing age. At this point, they were demolded and cut into 2-mm slices using a precision saw. These slices were then used for preparing the specimens for X-ray computed tomography. Hydration of the specimens was stopped by solvent exchange using isopropanol (Scrivener et al. 2016). Slices were immersed in the solution and taken out five times for a period of 60 s. This procedure was followed by 72 h of specimen immersion in isopropanol. Afterward, the specimens were taken out and the solvent removed by evaporation in ambient conditions. Specimens with hydration times of 7, 28, and 60 days were prepared.

X-Ray Computed Tomography

In order to perform X-ray computed tomography, microbeam specimens with a 500×500 μm cross section were prepared. Specimens were prepared for each w:c ratio and testing age. The specimen preparation procedure is described in detail in Zhang et al. (2017). Microbeams were then clamped by a holder and placed inside of the chamber of a CT scanning system (Phoenix Nanotom, Universal Systems, Manchester, New Hampshire) (Fig. 1). In total, 2,800 images were acquired on a digital GE DXR detector (Universal Systems, Manchester, New Hampshire) ($3{,}072 \times 2{,}400$ pixels) using a 12 keV/60 μA of X-ray source for a spatial resolution of $0.5 \times 0.5 \times 0.5$ μm. Phoenix datos|x CT software was used for reconstruction. In order to reduce the computational effort in the subsequent simulations, the original resolution was reduced to 2 μm after the reconstruction. The resulting image can then be used for phase segmentation: the grayscale value histogram can be segmented into four distinct phases: pore phase, outer hydration product phase, inner hydration product phase, and unhydrated cement phase. The segmentation procedure is described in detail in Zhang et al. (2016). A short description of the procedure is given here (Fig. 2): (1) the first inflection point in the cumulative fraction curve of grayscale values (T_1) was used to segment the solid phases; (2) a critical point at which a tangent slope of the histogram experiences a sudden change (T_2) was used to distinguish unhydrated cement from hydration products; and (3) the relative amount of the two hydration products (i.e., inner and outer product) was

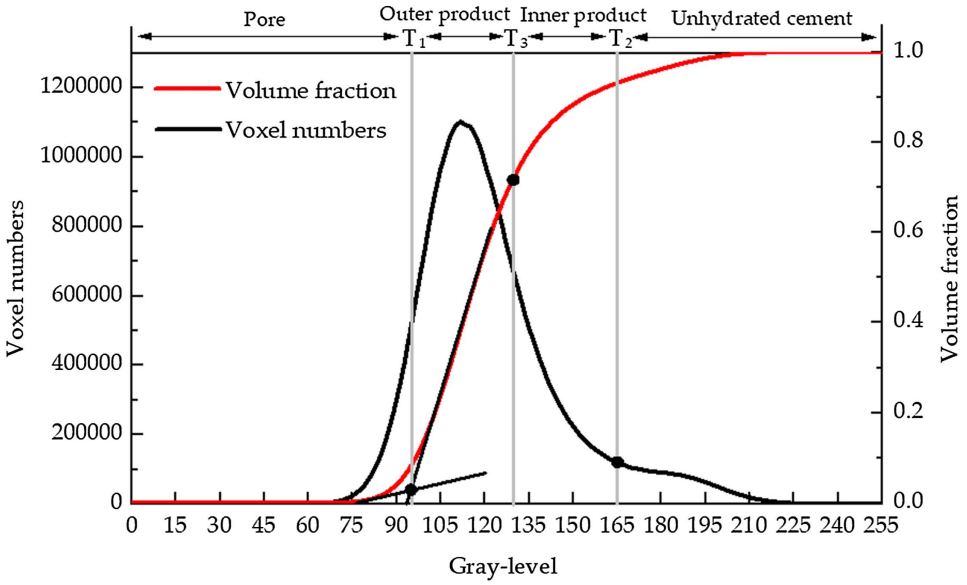

Fig. 2. Segmentation process of phases in cement paste based on grayscale value histogram of CT images. (Reprinted from *Cement and Concrete Research*, Vol. 102, H. Zhang, B. Šavija, S. Chaves Figueiredo, and E. Schlangen, "Experimentally validated multi-scale modelling scheme of deformation and fracture of cement paste," pp. 175–186, © 2017, with permission from Elsevier.)

J. Mater. Civ. Eng., 2019, 31(9): 04019169

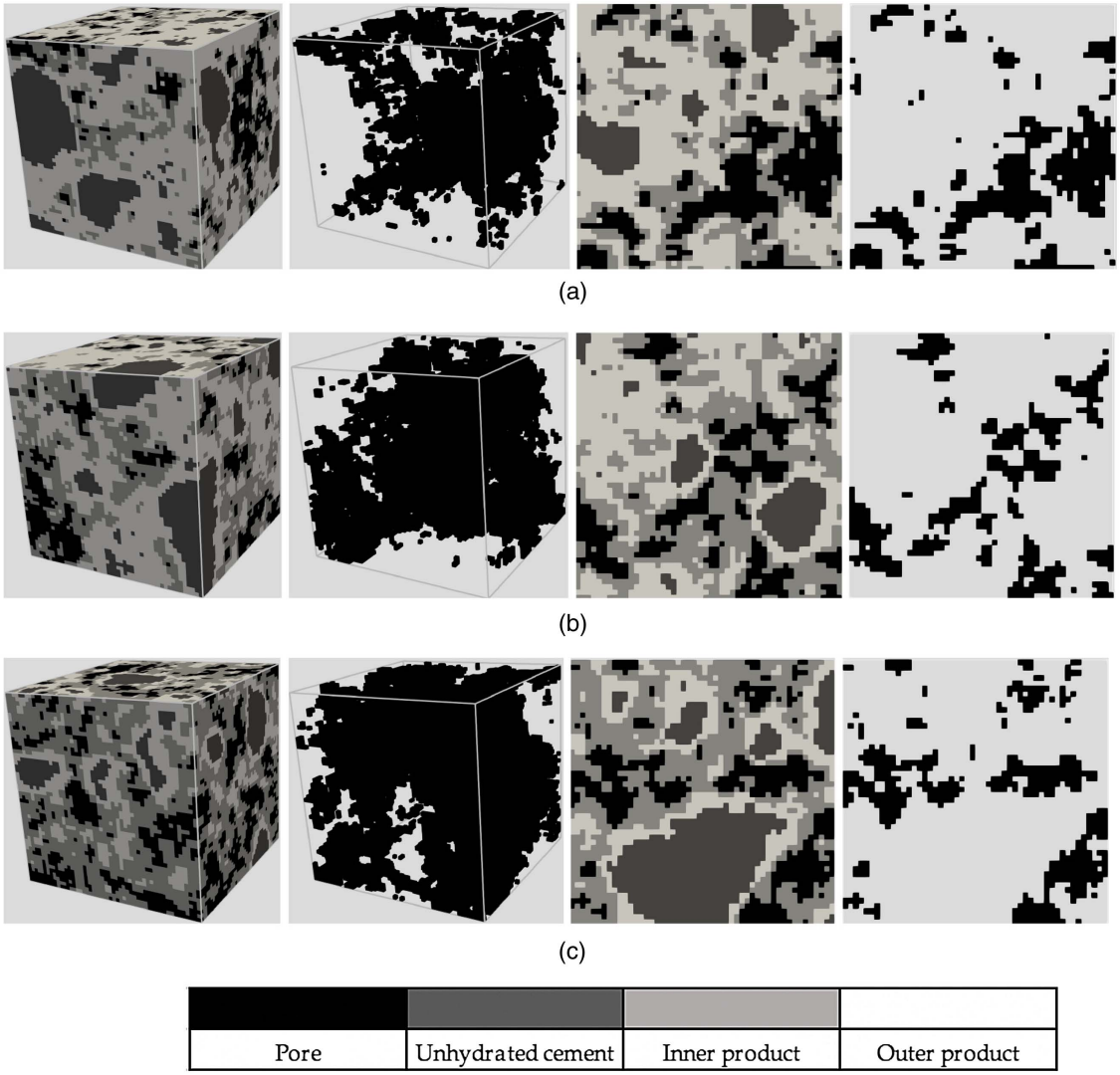

Fig. 3. Examples of 100 × 100 × 100 μm cement paste microcubes obtained from X-ray computed tomography after 7 days of hydration and subsequently segmented: (a) w:c = 0.3; (b) w:c = 0.4; and (c) w:c = 0.5.

subsequently adjusted to obtain their theoretical ratios (Tennis and Jennings 2000) by selecting a proper threshold point (T_3).

From each scanned image, 10 cubic subsamples of 100 × 100 × 100 μm (i.e., 50 × 50 × 50 voxels) were extracted to be used for numerical simulations. Examples of the microcubes are shown in Fig. 3 for 7 days and Fig. 4 for 60 days of hydration, respectively. Properties of each microcube were simulated in three orthogonal directions to capture the anisotropy in the material behavior. This provided 30 measures for the elastic modulus and chloride diffusivity for each w:c ratio and testing age.

Model Description

Discrete (lattice) models (Nikolić et al. 2018; Pan et al. 2018) have been used for more than two decades to simulate deformation and fracture in quasi-brittle materials such as concrete (Bolander and Sukumar 2005; Grassl et al. 2012; Schlangen and van Mier 1992), rock (Sands 2016; Schlangen and van Mier 1995), and nuclear graphite (Šavija et al. 2016, 2018). In recent years, discrete models have been also used to simulate transport processes in concrete (Abyaneh et al. 2014; Šavija et al. 2014; Wang and Ueda 2011). Furthermore, coupled mechanical and transport models, which consider the effect of cracking on transport, have been developed (Asahina et al. 2014; Benkemoun et al. 2017; Grassl and Bolander 2016; Luković et al. 2016). In the mechanical lattice model, the continuum is discretized as a set of truss or beam elements that can transfer forces. On the other hand, in the transport lattice model, the continuum is discretized as a set of one-dimensional conduit (pipe) elements through which the transport takes place.

The spatial domain is discretized as follows. First, the domain is divided into a number of cubic cells. A subcell is then defined in the middle of each cell. A node is generated randomly within each subcell using a pseudorandom number generator. This is followed by a Voronoi tessellation of the domain with respect to the defined nodes, wherein nodes in adjacent Voronoi cells are connected with lattice elements (Yip et al. 2005) [Fig. 5(a)]. The ratio between the subcell and the cell size controls the degree of randomness of the lattice. Introducing randomness is especially important for the fracture analysis, where it has been observed that a regular lattice results in crack patterns that are mesh dependent (Schlangen and Garboczi 1997). On the other hand, lattice randomness has no effect on the transport simulation results, as shown by Bolander and Berton (2004).

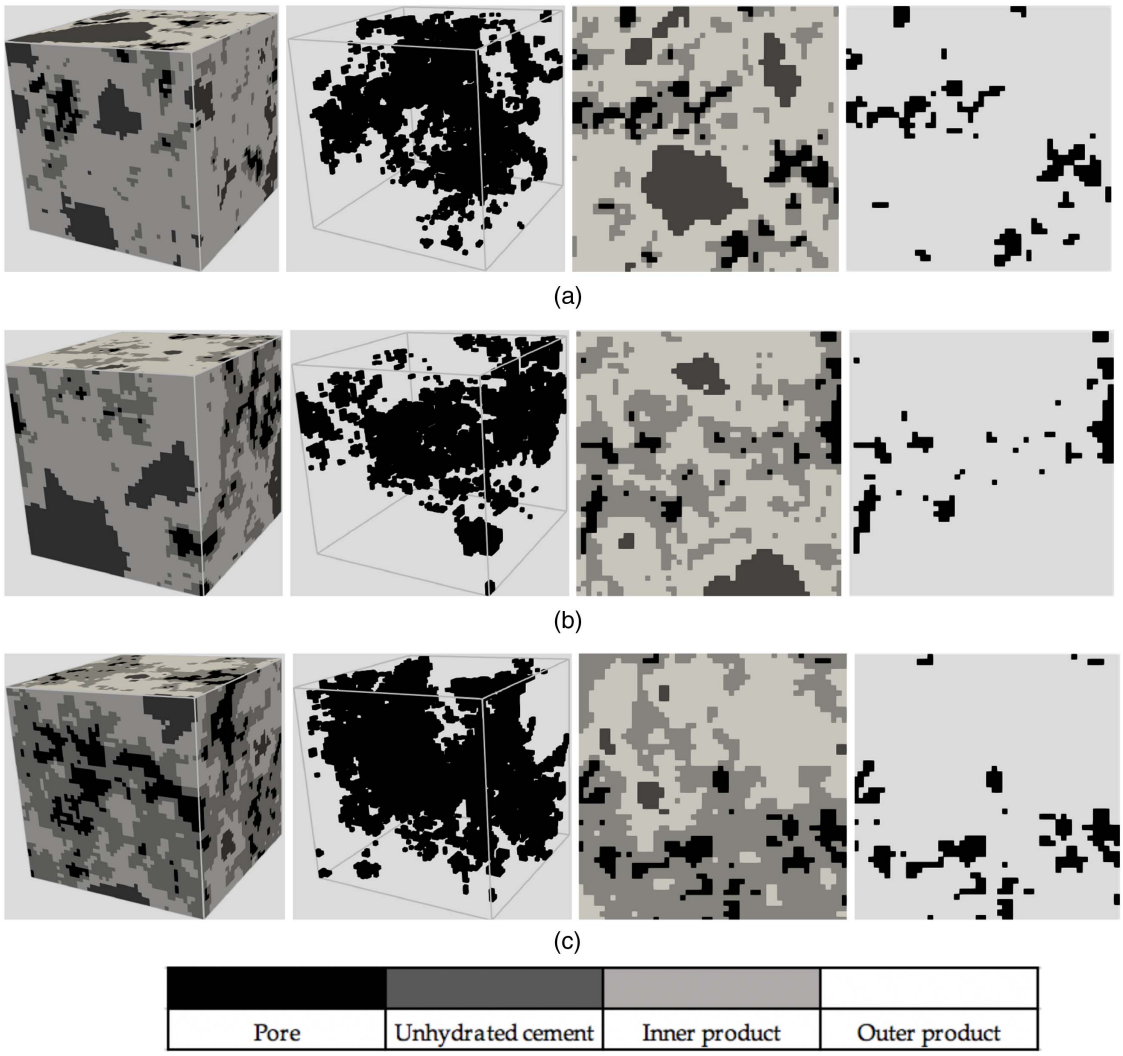

Fig. 4. Examples of $100 \times 100 \times 100$ μm cement paste microcubes obtained from X-ray computed tomography after 60 days of hydration and subsequently segmented: (a) w:c = 0.3; (b) w:c = 0.4; and (c) w:c = 0.5.

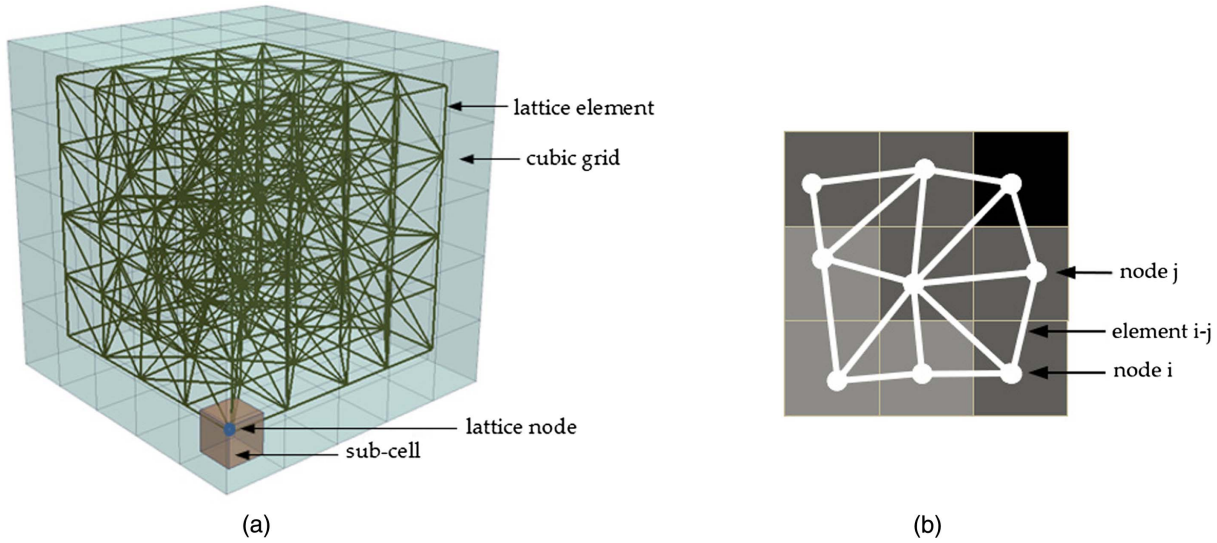

Fig. 5. (a) Node and mesh generation procedure; and (b) example of the overlay procedure for cement paste, shown in 2D for simplicity. (Shading used is the same as in Figs. 3 and 4.)

Material heterogeneity is easily considered in lattice models by utilizing the particle overlay procedure [Fig. 5(b)]. As input, either a computer-generated microstructure or a microstructure obtained by X-ray computed tomography can be used. Each node in the lattice mesh is assigned with a pixel-voxel value based on the material structure used. This is then used to define properties of each lattice element, which are made dependent on the pixel-voxel value of its end nodes. This way, different mechanical or transport properties can be assigned to different phases in the material.

Mechanical Lattice Model

In the Delft lattice model, the material is discretized as a set of Timoshenko beam elements (Schlangen and Qian 2009). These beams discretize the space as described. They are assigned to different phases present in the hydrated cement paste using the described overlay procedure. The elastic modulus of a lattice element $i-j$ connecting phases i and j is determined using a Reuss (series) model as (Zhang et al. 2016)

$$\frac{2}{E_{i-j}} = \frac{1}{E_i} + \frac{1}{E_j} \tag{1}$$

where E_i and E_j = elastic moduli corresponding to phases i and j, respectively. When either voxel i or voxel j is a pore voxel, no element is created in the lattice mesh.

For determining the elastic modulus of the paste, the specimen is subjected to a unit displacement on the one end, while it is clamped at the other end (Fig. 6). Since the material shows some anisotropy, this procedure is repeated for all three orthogonal directions, resulting in three measures of Young's modulus for each microcube.

For determination of the Young's modulus of cement paste, only Young's moduli of individual phases are needed as input (apart from the microstructure description, which is obtained by X-ray computed tomography in this work). Therefore, moduli obtained from nanoindentation experiments were used in this paper. Values for individual cement phases are given in Table 1.

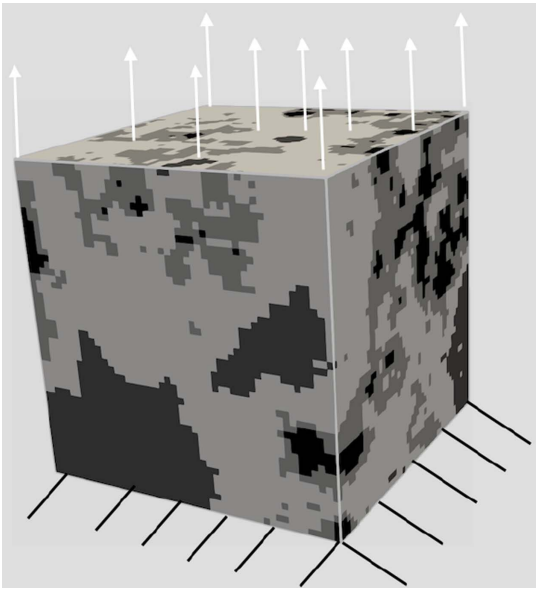

Fig. 6. Example of boundary conditions used for calculating the Young's modulus in the vertical (Y) direction. (Shading used is the same as in Figs. 3 and 4.) The boundaries are considered clamped (i.e., lateral contraction is restrained).

Table 1. Young's moduli measured by nanoindentation and used in the simulations

Phase	Young's modulus (GPa)
Unhydrated cement	99
Inner product	31
Outer product	25

Source: Data from Hu and Li (2014).

Lattice Transport Model

The lattice transport model treats concrete as an assembly of one-dimensional (1D) conduit (pipe) elements through which the chloride transport takes place. An assembly of these elements in a three-dimensional space enables simulation of transport in 3D. In the current study, chloride transport was assumed to be governed by diffusion only, i.e., water-saturated conditions were assumed. Furthermore, binding of chloride ions was not considered.

Chloride diffusivity of cement paste can be determined from steady-state diffusion experiments. Steady-state diffusion can be described by Fick's first law as (Garboczi 1990)

$$J = -D\frac{\partial C}{\partial x} \tag{2}$$

where J = flux of the diffusing species (chloride) per unit area; D = chloride diffusivity; C = chloride concentration; and x = spatial coordinate.

Eq. (2) can be discretized using the standard Galerkin procedure [for full derivation of the weak form of Fick's second law, of which Fick's first law is a special case, the reader is referred to Šavija et al. (2013)]. The following system of equations results (in matrix form):

$$\mathbf{KC} = \mathbf{f} \tag{3}$$

where $\mathbf{K}$ is the element diffusion matrix; and $\mathbf{f}$ is the forcing vector. Element matrices are given as

$$\mathbf{K} = \frac{DA}{l}\begin{bmatrix} 1 & -1 \\ -1 & 1 \end{bmatrix} \tag{4}$$

$$\mathbf{f} = \begin{bmatrix} -q_i A \\ -q_j A \end{bmatrix} \tag{5}$$

where A = uniform cross-sectional area of each 1D element; l and D = length and diffusion coefficient of each element; and q_i and q_j = prescribed nodal fluxes at nodes i and j. Cross-sectional areas of individual elements were determined using the so-called Voronoi scaling procedure (Yip et al. 2005). For each element, the cross-sectional area of an element was set equal to the facet of a Voronoi cell that was common to its end nodes (Fig. 7). Element matrices are the same as those of standard one-dimensional linear finite elements (Lewis et al. 2004).

Elements in the transport lattice mesh were assigned diffusion coefficients based on the voxel values of their end nodes [as described in Fig. 5(b)]. For each element $i-j$, the diffusion coefficient was determined as (Kamali-Bernard and Bernard 2009; Liu et al. 2013)

$$D_{i-j} = \frac{2}{\frac{1}{D_i} + \frac{1}{D_j}} \tag{6}$$

where D_i and D_j = diffusion coefficients of phases to which voxels at the end nodes (i and j, respectively) belong. Diffusion

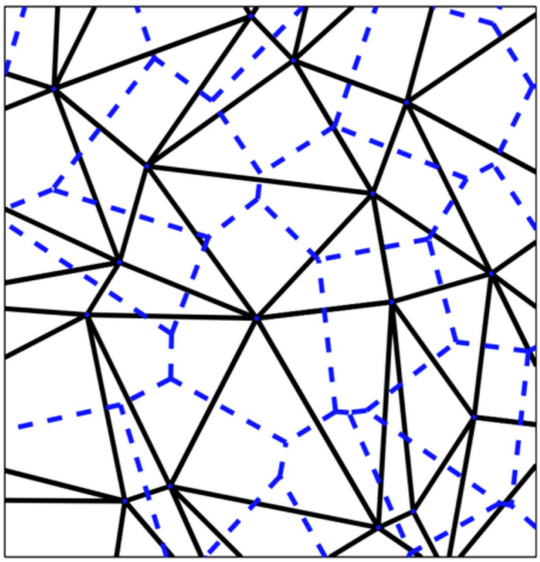

Fig. 7. Mesh of lattice elements (solid lines) with corresponding Voronoi tessellation (dashed lines).

coefficients of individual phases were set as follows (Liu et al. 2013): for pores, 1.07×10^{-10} m^2/s; for outer hydration product, 3.4×10^{-12} m^2/s; and for inner hydration product, 8.3×10^{-13} m^2/s. These values were determined using inverse analyses based on experimental data (Bary and Béjaoui 2006; Pivonka et al. 2004). Unhydrated cement particles were considered impermeable.

The diffusion coefficient of the material was calculated by solving the steady-state diffusion equation. In order to simulate a concentration gradient, fixed chloride concentrations were set at two opposing sides of the cubical domain (termed the inlet and the outlet, respectively). These values have been set to 1 (c_i) and 0 (c_o) mol/m^3, respectively. The chloride diffusion coefficient of the material can then be calculated as (Liu et al. 2013)

$$D_c = \frac{Q}{A_C}\frac{L_C}{c_i - c_o} \tag{7}$$

where Q = total flux through the outlet surface; L_C = length of the simulated sample; and A_C = its cross-sectional area perpendicular to the flow.

Results

Tomography Data

As the hydration process occurs, the microstructure of cement pastes evolves (see, e.g., changes in the microstructure between 7 days in Fig. 3 and 60 days in Fig. 4). This includes the evolution and refinement of the microstructure, reduction in the amount of unhydrated cement, and the proportion of hydration products. In this section, the microstructure and its evolution are studied based on X-ray computed tomography data.

For a volume of $200 \times 200 \times 200$ μm of each paste (i.e., three w:c ratios and three testing ages), pore size distribution was determined based on segmented X-ray computed tomography images. Calculation of pore size distribution was performed using a procedure presented by Dong et al. (2017). According to their procedure, pores with a diameter larger than twice the spatial resolution can be calculated. In the current case, therefore, the minimum pore size considered was 4 μm. Pore size distributions of all pastes are given in Fig. 8. It can be seen that, for all pastes, the volume of capillary pores decreased with curing age, which was expected (compare also Figs. 3 and 4). For pastes with higher w:c ratio (i.e., w:c = 0.4 and w:c = 0.5), there was a relatively large difference between the total porosity at 7 and at 28 days. For the low w:c ratio paste (i.e., paste with w:c = 0.3), this difference was much smaller. For all pastes, there was a decrease of porosity and a shift toward smaller pore sizes between 28 and 60 days.

The relative amount of each phase in the microstructure also evolved with time. For each w:c ratio and testing age, amounts of solid phases were calculated from X-ray tomography images (based on the segmentation procedure described) and are shown in Fig. 9. It can be seen, as expected, that the amount of unhydrated cement decreased with curing time for all w:c ratios. The low w:c (0.3) paste had the highest amount of unhydrated cement at all ages (which corresponds to the lowest degree of hydration as shown in Fig. 10). In terms of hydration products, the paste with a w:c = 0.3 had a relatively high proportion of inner product and a low proportion of the outer product. The paste with w:c = 0.5 showed an opposite trend: a high amount of outer hydration product and a relatively low amount of inner hydration product. These two hydration products had different porosities (i.e., gel porosities) (Jennings et al. 2007), which cannot be captured by X-ray computed tomography at the resolution used. They do, however, influence the elastic and transport properties of cement paste. The influence of the gel porosity was taken indirectly in simulations of elastic and diffusion properties, as described further.

Based on the X-ray tomography data, the degree of hydration of cement pastes can also be determined. The hydration degree is calculated by the following equation:

$$\text{DOH} = \frac{\frac{V_{\text{hydrated}}}{v}}{\frac{V_{\text{hydrated}}}{v} + V_{\text{unhydrated}}} \tag{8}$$

where DOH = degree of hydration; V_{hydrated} = volume of the hydration product; $V_{\text{unhydrated}}$ = volume of unhydrated cement; and v = ratio between the volume of the reaction product and the reactant. This ratio was taken to be 2.2 in this study (van Breugel 1997). The evolution of degree of hydration for the three w:c ratios based on X-ray computed tomography data is given in Fig. 10. It can be seen that the degree of hydration increased with age as expected, but that it was consistently lower for pastes with lower w:c ratios. For these pastes, it is expected that the effective properties will improve over a longer period of time.

Young's Modulus

Validation

The elastic modulus of cement paste depends on the porosity, the relative amounts of hydration products, and their elastic properties. In terms of the lattice simulation, the modulus may also depend on the resolution of input X-ray tomography images. In order to assess whether the proposed experimentally informed lattice model is capable of accurately predicting the elastic modulus of cement paste in spite of the limited X-ray computed tomography resolution used in the current study ($2 \times 2 \times 2$ μm), simulation results were first compared with data from the literature. The comparison is summarized in Fig. 11. In the work of Haecker et al. (2005), elastic moduli were determined using elastic resonance measurements, and the values they reported were an average of three replicate samples.

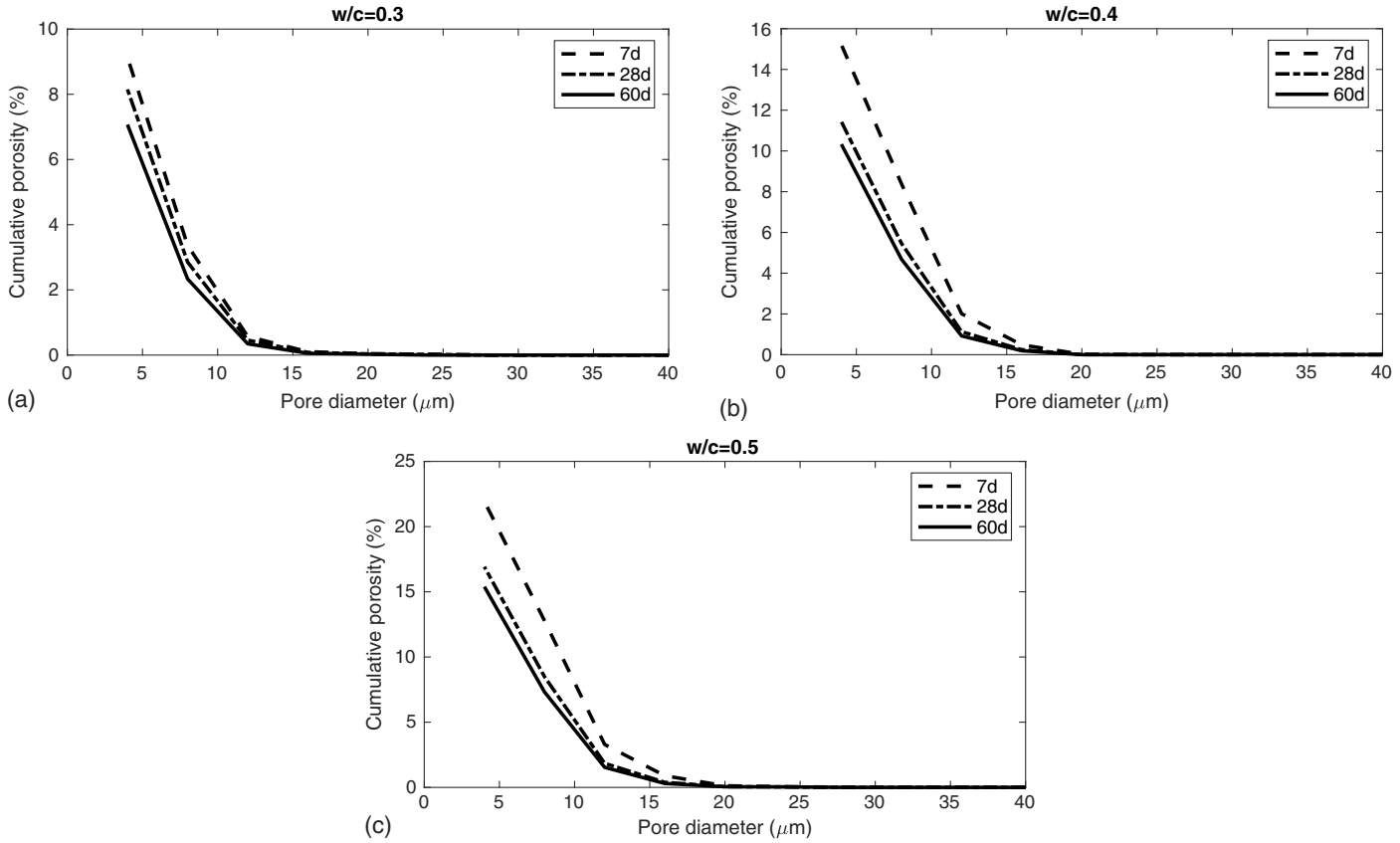

Fig. 8. Cumulative porosity of cement pastes calculated based on X-ray computed tomography data: (a) w:c = 0.3; (b) w:c = 0.4; and (c) w:c = 0.5.

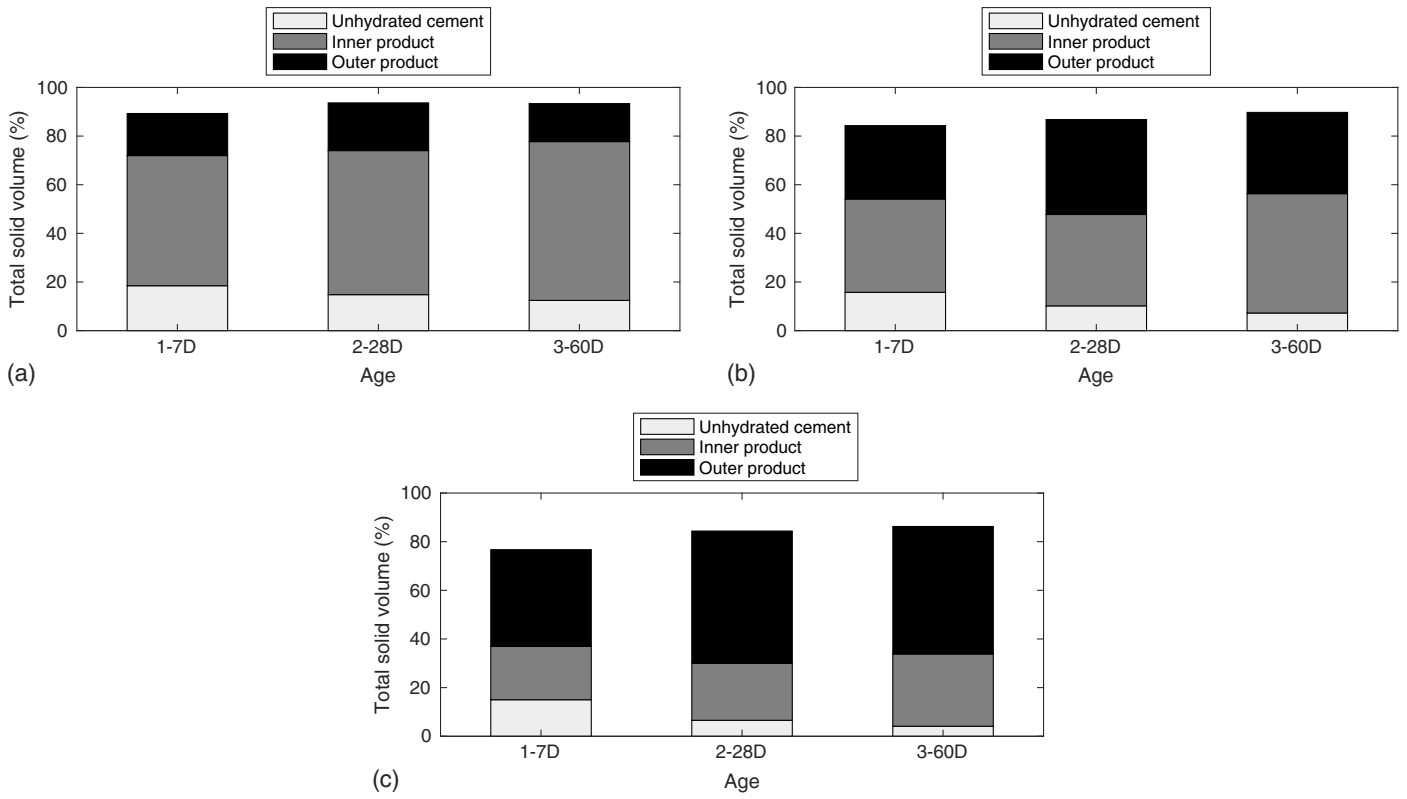

Fig. 9. Proportion of solid phases in cement pastes with different w:c ratios at different hydration ages based on X-ray computed tomography data: (a) w:c = 0.3; (b) w:c = 0.4; and (c) w:c = 0.5.

J. Mater. Civ. Eng., 2019, 31(9): 04019169

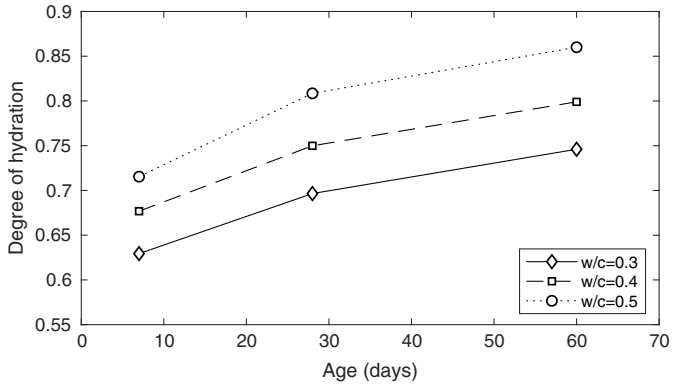

Fig. 10. Degree of hydration of cement pastes calculated based on X-ray computed tomography data.

It can be clearly seen that, when compared with experimental measurements of Haecker et al. (2005), the model showed an excellent fit. The model also performed very well compared to the model of Zhang and Jivkov (2016), although a much more detailed input (with a spatial resolution of $0.5 \times 0.5 \times 0.5$ μm) was used to feed their bond-site model. On the other hand, it is clear that the results of Qian (2012) show significantly lower values compared to other studies. Qian (2012) used a computer-generated microstructure as input for his mechanical model, which could potentially be an oversimplification of the real microstructure in terms of morphology. This is a clear improvement of the experimentally informed procedure: no assumptions were made in creating the microstructure, thereby resulting in more accurate model predictions.

Property Development

Development of Young's modulus with time simulated using the experimentally informed lattice model is shown in Fig. 12. Results obtained by numerical simulations of Zhang and Jivkov (2016) are given for comparison. It can be seen that, as expected, the Young's modulus increased with curing age for all considered w:c ratios. This is a result of the continued microstructure development, which is characterized by higher degree of hydration (Fig. 10), decrease in porosity (Fig. 8), and the resulting increase in volume of strength-contributing solids (Fig. 9). Furthermore, it can be seen that the

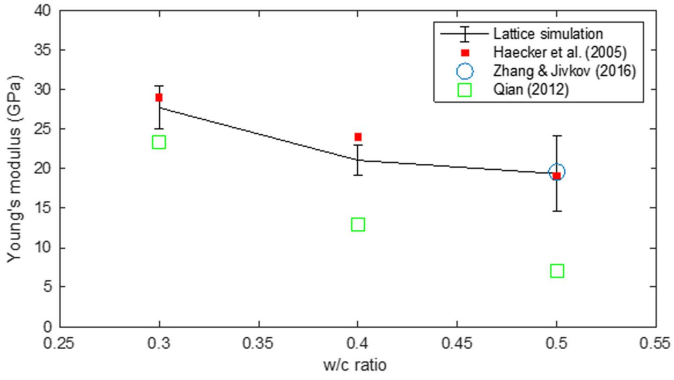

Fig. 11. Young's modulus of cement pastes cured for 28 days calculated using experimentally informed lattice model compared with literature data. Error bars indicate standard deviation. For each parameter (w:c, age), 30 simulations were performed (10 microstructures in three orthogonal directions). Filled symbols indicate experimental values and open symbols were obtained by other numerical models.

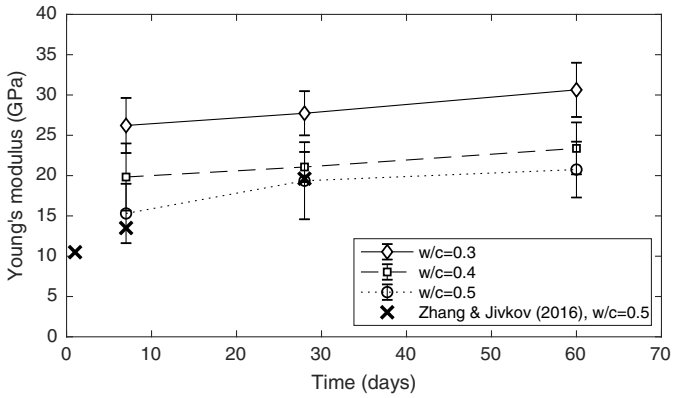

Fig. 12. Development of Young's modulus for hydrated cement paste with different w:c ratios determined using experimentally informed lattice model. Error bars indicate standard deviation. For each parameter (w:c, age), 30 simulations were performed (10 microstructures in three orthogonal directions). Results from Zhang and Jivkov (2016) simulation are given for comparison.

proposed experimentally informed lattice model showed results comparable to those of Zhang and Jivkov (2016), who used a much higher resolution in their simulations.

Fig. 13 plots the simulated Young's moduli for all microcubes as a function of the total porosity.

The Young's modulus of cement paste is approximately an exponential function of the porosity, i.e., of the following form:

$$E = ae^{bP} \tag{9}$$

where E = Young's modulus of cement paste (GPa); a and b = fitting parameters; and P = porosity (%). For the considered cement pastes, the fitting coefficients were $a = 38.76$ and $b = -0.04418$ and the coefficient of determination was $R^2 = 0.9337$. The exponential fit is valid for all w:c ratios and ages: in other words, the Young's modulus of considered cement pastes is dominantly a function of porosity. Relative amounts of solids (i.e., unhydrated particles and hydration products) in the skeleton is of secondary importance for the Young's modulus of the composite according to the model since the Young's moduli of individual hydration phases are relatively similar, especially the inner and the outer product, while the amount of unhydrated cement is small. An exponential relation between porosity and Young's modulus has been proposed previously in the literature. For example, Spriggs (1961)

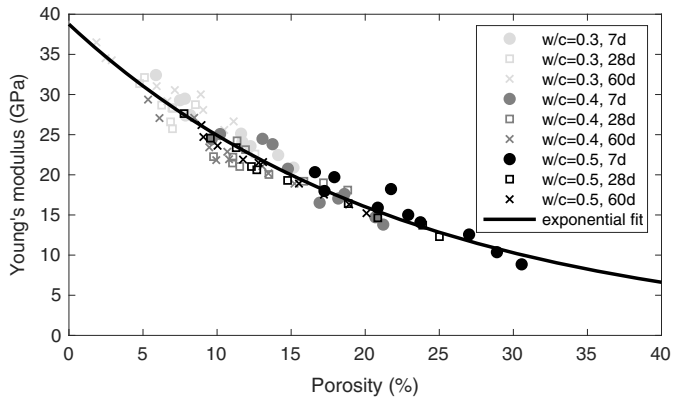

Fig. 13. Young's modulus as a function of total porosity.

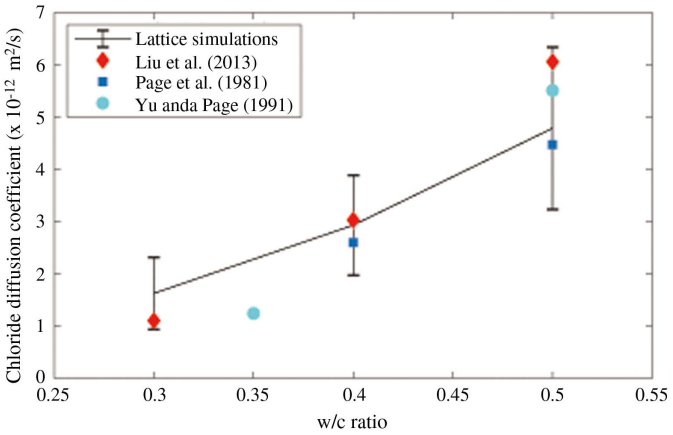

Fig. 14. Chloride diffusion coefficient calculated using experimentally informed lattice model compared with literature data. Error bars indicate standard deviation.

showed that the relation is valid for refractory materials. This relation is purely empirical and, although it is valid for a practical range of porosities, it does not satisfy the physical condition that, for a 100% porosity, a zero elastic modulus should be obtained (Hasselman 1962).

Diffusivity

Validation

The resolution of X-ray tomography scans that were used as input in the model was limited. This resulted in neglecting the influence of smaller pores on the transport, although gel porosity in the hydration products was implicitly considered through their transport properties. In order to test whether the proposed discrete model is able to accurately determine the diffusion coefficient of cement paste, simulation results were first compared with results from the literature. Liu et al. (2013) used simulated microstructures to calculate the chloride diffusivity of cement paste. For model validation, they collected experimental results from the literature wherein chloride diffusion of cement pastes was determined by steady-state diffusion tests. Two of these studies were selected as experimental benchmarks (Page et al. 1981; Yu and Page 1991). Page et al. (1981) performed chloride diffusion tests at the age of 60 days, while Yu and Page (1991) performed the tests at 90–810 days of hydration. On the other hand, Liu et al.'s (2013) simulations were performed using hydrated cement pastes after 83 days of hydration as input. Furthermore, they performed a single simulation for each w:c ratio. A comparison between lattice simulations and literature data is given in Fig. 14. An example visualization of the simulation result is given in Fig. 15.

It can be seen that the model was able to predict the experimentally observed chloride diffusion coefficient of cement pastes quite accurately. Furthermore, there was an excellent match with the simulation results of Liu et al. (2013). This is worth noting since they used a much finer voxel size ($0.5 \times 0.5 \times 0.5$ μm) compared to the experimentally informed model ($2 \times 2 \times 2$ μm). If the same numerical procedure would be used, this would essentially mean that the number of degrees of freedom in the system was $4^3 = 64$ times smaller, which is very significant in terms of computational time. Again, the only difference between the two models was the microstructural input (diffusion coefficients of individual

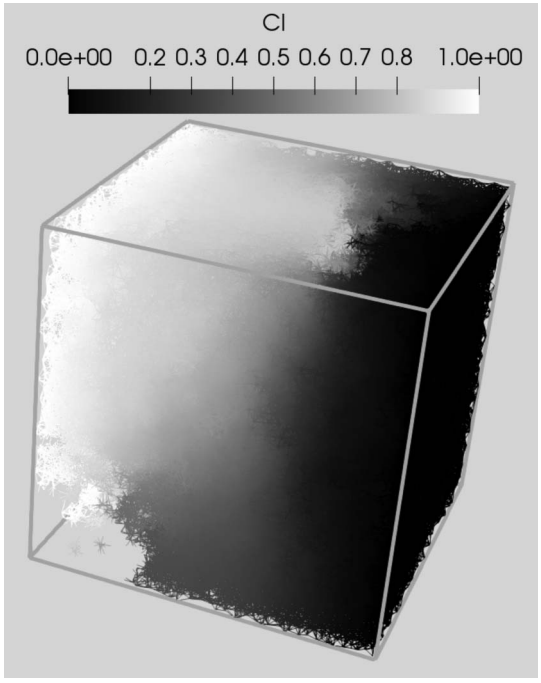

Fig. 15. Chloride distribution in cement paste under an imposed concentration gradient in the Z-direction.

phases are the same in the two models): while Liu et al. (2013) used a computer-generated microstructure [i.e., using HYMOSTRUC3D (Ye 2005)], a real microstructure was used in this research. This results in an improved description of the microstructure and, consequently, improved simulations.

Property Development

The development of chloride diffusivity of cement pastes with hydration time is given in Fig. 16. As expected, the chloride diffusivity decreased with hydration time due to the microstructure evolution and pore structure refinement. This decrease was more significant for the period between 7 and 28 days and for a higher w:c ratio. This is consistent with the development of degree of

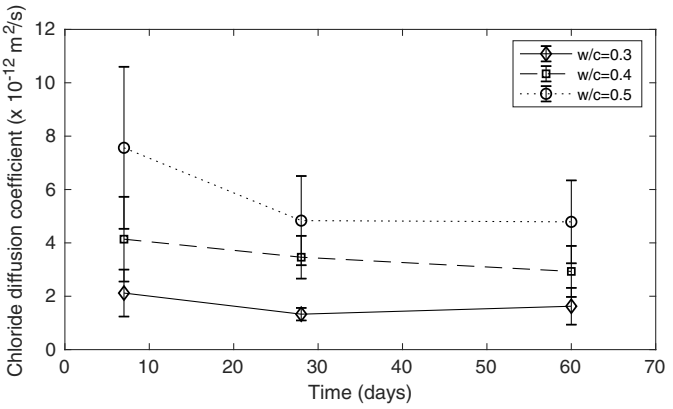

Fig. 16. Development of chloride diffusion coefficient for hydrated cement paste with different w:c ratios determined using experimentally informed lattice model. Error bars indicate standard deviation. For each parameter (w:c, age), 30 simulations were performed (10 microstructures in three orthogonal directions).

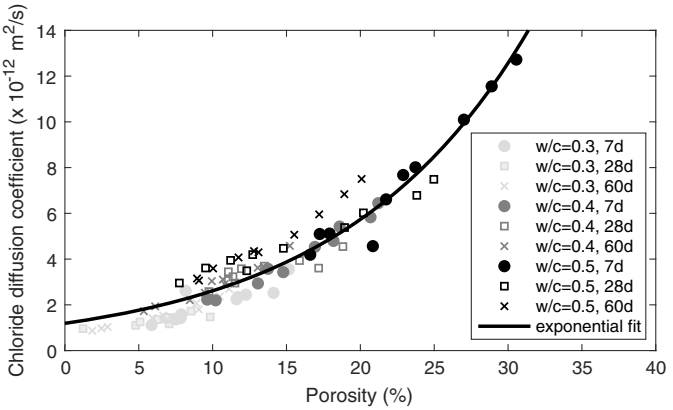

Fig. 17. Chloride diffusion coefficient as a function of total porosity. For each small cube, an average value of the chloride diffusion coefficient in three orthogonal directions is plotted.

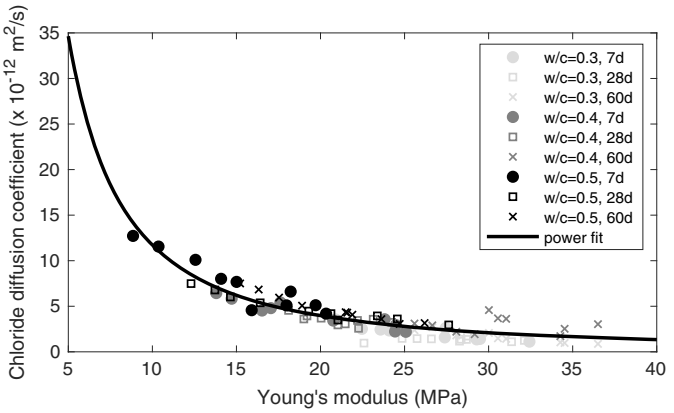

Fig. 18. Relationship between Young's modulus and chloride diffusion coefficient for hydrated cement pastes considered. For $E = 0$, the diffusion coefficient according to Eq. (11) is equal to 4.293×10^{-10} m^2/s, which is of the same order of magnitude as the chloride diffusion coefficient in the pore solution (1.07×10^{-10} m^2/s).

hydration (Fig. 10). Although not a lot of data are available in the literature for cement paste, a similar trend was observed for mortar (Caballero et al. 2012), where chloride diffusivity at early and later ages was measured using rapid chloride migration tests.

In Fig. 17, chloride diffusion coefficient for all microcubes is plotted as a function of total porosity.

It can be seen from Fig. 17 that the chloride diffusion coefficient of hydrated cement paste was dependent on the porosity in an approximately exponential way. An exponential relation between the porosity and the chloride diffusion coefficient was determined through regression analysis as follows:

$$D = ae^{bP} \tag{10}$$

where D = diffusion coefficient (10^{-12} m^2/s); a and b = fitting parameters; and P = porosity (%). For the considered cement pastes, $a = 1.192$ and $b = 0.07852$, with a coefficient of determination $R^2 = 0.9164$. The exponential fit is also shown in Fig. 17.

Discussion

It is clear that both the Young's modulus and the chloride diffusivity of hydrated portland cement paste are dependent on the microstructure, especially the porosity. However, while the Young's modulus decreases exponentially with increasing porosity (Fig. 13), the chloride diffusion coefficient shows an exponential increase with increasing porosity (Fig. 17). Therefore, for the ordinary portland cement pastes considered, it may be possible to define a relationship between the Young's modulus and the chloride diffusion coefficient. Fig. 18 plots a relationship between the calculated Young's modulus and calculated chloride diffusion coefficient for each microcube.

It can be seen that an approximately power relation exists between the two variables. This relation can be written as

$$D = kE^m \tag{11}$$

where k and m = fitting parameters. For the microstructures considered, $k = 429.3$ and $m = -1.564$, and the power fit had a coefficient of determination $R^2 = 0.8534$. The fitting relation is also shown in Fig. 18.

Although it is commonly stated that durability properties of concrete (which, apart from cement paste, also constitutes the interfacial transition zone and aggregate phases) should not be determined by correlations with mechanical properties, the existence of such a relationship for portland cement paste is not completely unexpected. For example, Moon et al. (2006) found a linear relationship between chloride diffusivity and compressive strength of portland cement concrete. However, a much weaker correlation was found for concretes with blended cements. They attributed this to "the differences of the pore characteristics like the distribution of pore diameters between both portland and blended cements concretes, which affect the compressive strength and chloride diffusivity" (Moon et al. 2006). Therefore, an exponential (or in this case a power) relation between porosity and diffusivity is not unexpected. However, the relationship proposed in this paper is probably not universal, and it may be different for blended cements. In addition, since the contribution of small pores (smaller than 2 μm) was not considered explicitly in the model, a multiscale strategy [such as that proposed by, e.g., Ma et al. (2015)] may need to be employed for systems with very fine pore structures such as blended cements.

Summary and Conclusions

In this paper, an experimentally informed modeling approach for determining elastic (Young's modulus) and transport (chloride diffusivity) properties has been proposed. The models use X-ray computed tomography data as microstructural input, describing the pore structure and the morphology in a way that is more realistic compared to most microstructural models. Both the mechanical and the transport model use a discrete (lattice) approach to discretize the material domain and simulate different phases in the microstructure. The models need a limited number of input parameters: elastic properties of cement phases for the mechanical model and diffusion coefficients of cement phases for the transport model. While in this research these have been based on literature data, in principle lower scale models [such as molecular dynamics (Pellenq et al. 2009; Zehtab and Tarighat 2018)] can be used to determine the input parameters. First, the validity of the models has been shown by comparing the results with data available from the literature. Second, microstructure-property relationships and their time dependence were explored. Finally, a correlation between Young's modulus and chloride diffusivity in ordinary portland cement pastes has been discussed. Based on the presented results, the following conclusions can be drawn:

- Proposed experimentally informed discrete models are able to correctly predict properties compared with the available literature. This is especially striking given the limited spatial resolution of X-ray tomography data that were used as input.
- Modeling results reflect the time evolution of the evaluated mechanical and transport properties.
- According to the models, both the Young's modulus and the diffusion coefficient are primarily a function of the total porosity (in the range studied). While the Young's modulus decreased exponentially with increasing porosity, the chloride diffusion coefficient showed an exponential increase.
- For the portland cement pastes considered in this study, the models showed a correlation between the Young's modulus and the chloride diffusion coefficient. Although this is in accordance with some literature data, the validity of such correlation should not be extended beyond the scope of this study (to consider, e.g., blended cements).

Although the models show excellent results, a number of simplifying assumptions have been made. First, due to the limited resolution of the scans, small capillary pores and all gel pores were not considered. As a consequence, the diffusivity determined by the model was only a function of the total porosity, while effects of pore connectivity and tortuosity were masked by the limited resolution of the input. Second, properties of individual cement phases (e.g., inner and outer hydration product) were assumed to be constant over time. These issues could be resolved by correlating the grayscale value from the X-ray tomography directly with the cement paste mechanical and transport properties, which would then not require phase segmentation but would include the influence of gel pores. This approach is currently being developed for determining the mechanical properties of cement paste (Zhang et al. 2019). And third, in simulating chloride diffusivity, steady-state conditions were assumed and chloride binding was not considered. In the future, all these aspects will have to be considered, e.g., by using multiscale modeling, in order to make the models more robust.

Data Availability Statement

Data used and created in this research are available on request.

Acknowledgments

This work has been financially supported by an European Union Horizon 2020 project InnovaConcrete (Innovative Materials and Techniques for the Conservation of 20th Century Concrete-Based Cultural Heritage), Grant Agreement Number 760858. Hongzhi Zhang would like to acknowledge the financial support of the China Scholarship Council (CSC) under Grant CSC No. 201506120067. Arjan Thijssen performed the X-ray computed tomography experiments and his assistance is gratefully acknowledged.

References

Abyaneh, S. D., H. Wong, and N. Buenfeld. 2014. "Computational investigation of capillary absorption in concrete using a three-dimensional mesoscale approach." *Comput. Mater. Sci.* 87: 54–64. https://doi.org/10.1016/j.commatsci.2014.01.058.

Asahina, D., J. E. Houseworth, J. T. Birkholzer, J. Rutqvist, and J. Bolander. 2014. "Hydro-mechanical model for wetting/drying and fracture development in geomaterials." *Comput. Geosci.* 65: 13–23. https://doi.org/10.1016/j.cageo.2013.12.009.

Bary, B., and S. Béjaoui. 2006. "Assessment of diffusive and mechanical properties of hardened cement pastes using a multi-coated sphere assemblage model." *Cem. Concr. Res.* 36 (2): 245–258. https://doi.org/10.1016/j.cemconres.2005.07.007.

Benkemoun, N., M. N. Hammood, and O. Amiri. 2017. "A meso-macro numerical approach for crack-induced diffusivity evolution in concrete." *Constr. Build. Mater.* 141: 72–85. https://doi.org/10.1016/j.conbuildmat.2017.02.146.

Bentz, D. P. 2006. "Quantitative comparison of real and CEMHYD3D model microstructures using correlation functions." *Cem. Concr. Res.* 36 (2): 259–263. https://doi.org/10.1016/j.cemconres.2005.07.003.

Bishnoi, S., and K. L. Scrivener. 2009. "μic: A new platform for modelling the hydration of cements." *Cem. Concr. Res.* 39 (4): 266–274. https://doi.org/10.1016/j.cemconres.2008.12.002.

Bolander, J. E. Jr., and S. Berton. 2004. "Simulation of shrinkage induced cracking in cement composite overlays." *Cem. Concr. Compos.* 26 (7): 861–871. https://doi.org/10.1016/j.cemconcomp.2003.04.001.

Bolander, J. E., and N. Sukumar. 2005. "Irregular lattice model for quasi-static crack propagation." *Phys. Rev. B* 71 (9): 094106. https://doi.org/10.1103/PhysRevB.71.094106.

Caballero, J., R. B. Polder, G. A. Leegwater, and A. L. Fraaij. 2012. "Chloride penetration into cementitious mortar at early age." *Heron* 57 (3): 185–196.

Çopuroğlu, O., and E. Schlangen. 2008. "Modeling of frost salt scaling." *Cem. Concr. Res.* 38 (1): 27–39. https://doi.org/10.1016/j.cemconres.2007.09.003.

Damrongwiriyanupap, N., S. Scheiner, B. Pichler, and C. Hellmich. 2017. "Self-consistent channel approach for upscaling chloride diffusivity in cement pastes." *Transp. Porous Med.* 118 (3): 495–518. https://doi.org/10.1007/s11242-017-0867-3.

Dong, H., P. Gao, and G. Ye. 2017. "Characterization and comparison of capillary pore structures of digital cement pastes." *Mater. Struct.* 50 (2): 154. https://doi.org/10.1617/s11527-017-1023-9.

Gallucci, E., K. Scrivener, A. Groso, M. Stampanoni, and G. Margaritondo. 2007. "3D experimental investigation of the microstructure of cement pastes using synchrotron X-ray microtomography (μCT)." *Cem. Concr. Res.* 37 (3): 360–368. https://doi.org/10.1016/j.cemconres.2006.10.012.

Garboczi, E. J. 1990. "Permeability, diffusivity, and microstructural parameters: A critical review." *Cem. Concr. Res.* 20 (4): 591–601. https://doi.org/10.1016/0008-8846(90)90101-3.

Grassl, P., and J. Bolander. 2016. "Three-dimensional network model for coupling of fracture and mass transport in quasi-brittle geomaterials." *Materials* 9 (9): 782. https://doi.org/10.3390/ma9090782.

Grassl, P., D. Grégoire, L. R. Solano, and G. Pijaudier-Cabot. 2012. "Meso-scale modelling of the size effect on the fracture process zone of concrete." *Int. J. Solids Struct.* 49 (13): 1818–1827. https://doi.org/10.1016/j.ijsolstr.2012.03.023.

Haecker, C.-J., E. Garboczi, J. Bullard, R. Bohn, Z. Sun, S. Shah, and T. Voigt. 2005. "Modeling the linear elastic properties of portland cement paste." *Cem. Concr. Res.* 35 (10): 1948–1960. https://doi.org/10.1016/j.cemconres.2005.05.001.

Hasselman, D. 1962. "On the porosity dependence of the elastic moduli of polycrystalline refractory materials." *J. Am. Ceram. Soc.* 45 (9): 452–453. https://doi.org/10.1111/j.1151-2916.1962.tb11191.x.

Hirsch, T. J. 1962. "Modulus of elasticity of concrete affected by elastic moduli of cement paste matrix and aggregate." *ACI J. Proc.* 59 (3): 427–452.

Hu, C., and Z. Li. 2014. "Micromechanical investigation of portland cement paste." *Constr. Build. Mater.* 71: 44–52. https://doi.org/10.1016/j.conbuildmat.2014.08.017.

Jennings, H. M., J. J. Thomas, J. S. Gevrenov, G. Constantinides, and F.-J. Ulm. 2007. "A multi-technique investigation of the nanoporosity of cement paste." *Cem. Concr. Res.* 37 (3): 329–336. https://doi.org/10.1016/j.cemconres.2006.03.021.

Kamali-Bernard, S., and F. Bernard. 2009. "Effect of tensile cracking on diffusivity of mortar: 3D numerical modelling." *Comput. Mater. Sci.* 47 (1): 178–185. https://doi.org/10.1016/j.commatsci.2009.07.005.

Lewis, R. W., P. Nithiarasu, and K. N. Seetharamu. 2004. *Fundamentals of the finite element method for heat and fluid flow.* West Sussex, UK: Wiley.

Liu, C., R. Huang, Y. Zhang, Z. Liu, and M. Zhang. 2018. "Modelling of irregular-shaped cement particles and microstructural development of portland cement." *Constr. Build. Mater.* 168: 362–378. https://doi.org/10.1016/j.conbuildmat.2018.02.142.

Liu, L., H. Chen, W. Sun, and G. Ye. 2013. "Microstructure-based modeling of the diffusivity of cement paste with micro-cracks." *Constr. Build. Mater.* 38: 1107–1116. https://doi.org/10.1016/j.conbuildmat.2012.10.002.

Luković, M., B. Šavija, H. Dong, E. Schlangen, and G. Ye. 2014. "Micromechanical study of the interface properties in concrete repair systems." *J. Adv. Concr. Technol.* 12 (9): 320–339. https://doi.org/10.3151/jact.12.320.

Luković, M., B. Šavija, E. Schlangen, G. Ye, and K. van Breugel. 2016. "A 3D lattice modelling study of drying shrinkage damage in concrete repair systems." *Materials* 9 (7): 575. https://doi.org/10.3390/ma9070575.

Ma, H., D. Hou, and Z. Li. 2015. "Two-scale modeling of transport properties of cement paste: Formation factor, electrical conductivity and chloride diffusivity." *Comput. Mater. Sci.* 110: 270–280. https://doi.org/10.1016/j.commatsci.2015.08.048.

Montero-Chacón, F., J. Marín-Montín, and F. Medina. 2014. "Mesomechanical characterization of porosity in cementitious composites by means of a voxel-based finite element model." *Comput. Mater. Sci.* 90: 157–170. https://doi.org/10.1016/j.commatsci.2014.03.066.

Moon, H. Y., H. S. Kim, and D. S. Choi. 2006. "Relationship between average pore diameter and chloride diffusivity in various concretes." *Constr. Build. Mater.* 20 (9): 725–732. https://doi.org/10.1016/j.conbuildmat.2005.02.005.

Nikolić, M., E. Karavelić, A. Ibrahimbegovic, and P. Miščević. 2018. "Lattice element models and their peculiarities." *Arch. Comput. Methods Eng.* 25 (3): 753–784. https://doi.org/10.1007/s11831-017-9210-y.

Page, C., N. Short, and A. El Tarras. 1981. "Diffusion of chloride ions in hardened cement pastes." *Cem. Concr. Res.* 11 (3): 395–406. https://doi.org/10.1016/0008-8846(81)90111-3.

Pan, Z., R. Ma, D. Wang, and A. Chen. 2018. "A review of lattice type model in fracture mechanics: Theory, applications, and perspectives." *Eng. Fract. Mech.* 190: 382–409. https://doi.org/10.1016/j.engfracmech.2017.12.037.

Pellenq, R. J.-M., A. Kushima, R. Shahsavari, K. J. Van Vliet, M. J. Buehler, S. Yip, and F.-J. Ulm. 2009. "A realistic molecular model of cement hydrates." *Proc. Natl. Acad. Sci. U. S. A.* 106 (38): 16102–16107. https://doi.org/10.1073/pnas.0902180106.

Pichler, B., C. Hellmich, and J. Eberhardsteiner. 2009. "Spherical and acicular representation of hydrates in a micromechanical model for cement paste: Prediction of early-age elasticity and strength." *Acta Mech.* 203 (3–4): 137. https://doi.org/10.1007/s00707-008-0007-9.

Pivonka, P., C. Hellmich, and D. Smith. 2004. "Microscopic effects on chloride diffusivity of cement pastes—A scale-transition analysis." *Cem. Concr. Res.* 34 (12): 2251–2260. https://doi.org/10.1016/j.cemconres.2004.04.010.

Powers, T. C., and T. L. Brownyard. 1946."Studies of the physical properties of hardened portland cement paste." *ACI J. Proc.*, 43 (9): 249–339.

Qian, Z. 2012. "*Multiscale modeling of fracture processes in cementitious materials*." Ph.D. thesis, Faculty of Civil Engineering and Geosciences, Dept. of structural Engineering, Delft Univ. of Technology.

Sands, C. M. 2016. "An irregular lattice model to simulate crack paths in bonded granular assemblies." *Comput. Struct.* 162: 91–101. https://doi.org/10.1016/j.compstruc.2015.09.006.

Šavija, B., D. Liu, G. Smith, K. R. Hallam, E. Schlangen, and P. E. Flewitt. 2016. "Experimentally informed multi-scale modelling of mechanical properties of quasi-brittle nuclear graphite." *Eng. Fract. Mech.* 153: 360–377. https://doi.org/10.1016/j.engfracmech.2015.10.043.

Šavija, B., M. Luković, and E. Schlangen. 2014. "Lattice modeling of rapid chloride migration in concrete." *Cem. Concr. Res.* 61–62: 49–63. https://doi.org/10.1016/j.cemconres.2014.04.004.

Šavija, B., J. Pacheco, and E. Schlangen. 2013. "Lattice modeling of chloride diffusion in sound and cracked concrete." *Cem. Concr. Compos.* 42: 30–40. https://doi.org/10.1016/j.cemconcomp.2013.05.003.

Šavija, B., G. E. Smith, P. J. Heard, E. Sarakinou, J. E. Darnbrough, K. R. Hallam, E. Schlangen, and P. E. Flewitt. 2018. "Modelling deformation and fracture of Gilsocarbon graphite subject to service environments." *J. Nucl. Mater.* 499: 18–28. https://doi.org/10.1016/j.jnucmat.2017.10.076.

Schlangen, E., and E. Garboczi. 1997. "Fracture simulations of concrete using lattice models: Computational aspects." *Eng. Fract. Mech.* 57 (2–3): 319–332. https://doi.org/10.1016/S0013-7944(97)00010-6.

Schlangen, E., and Z. Qian. 2009. "3D modeling of fracture in cement-based materials." *J. Multiscale Model.* 1 (2): 245–261. https://doi.org/10.1142/S1756973709000116.

Schlangen, E., and J. van Mier. 1992. "Simple lattice model for numerical simulation of fracture of concrete materials and structures." *Mater. Struct.* 25 (9): 534–542. https://doi.org/10.1007/BF02472449.

Schlangen, E., and J. van Mier. 1995. "Crack propagation in sandstone: Combined experimental and numerical approach." *Rock Mech. Rock Eng.* 28 (2): 93–110. https://doi.org/10.1007/BF01020063.

Scrivener, K., R. Snellings, and B. Lothenbach. 2016. *A practical guide to microstructural analysis of cementitious materials.* Boca Raton: CRC Press.

Sherzer, G., P. Gao, E. Schlangen, G. Ye, and E. Gal. 2017. "Upscaling cement paste microstructure to obtain the fracture, shear, and elastic concrete mechanical LDPM parameters." *Materials* 10 (3): 242. https://doi.org/10.3390/ma10030242.

Spriggs, R. 1961. "Expression for effect of porosity on elastic modulus of polycrystalline refractory materials, particularly aluminum oxide." *J. Am. Ceram. Soc.* 44 (12): 628–629. https://doi.org/10.1111/j.1151-2916.1961.tb11671.x.

Tennis, P. D., and H. M. Jennings. 2000. "A model for two types of calcium silicate hydrate in the microstructure of portland cement pastes." *Cem. Concr. Res.* 30 (6): 855–863. https://doi.org/10.1016/S0008-8846(00)00257-X.

Toutanji, H. A., and T. El-Korchi. 1995. "The influence of silica fume on the compressive strength of cement paste and mortar." *Cem. Concr. Res.* 25 (7): 1591–1602. https://doi.org/10.1016/0008-8846(95)00152-3.

van Breugel, K. 1997. "Simulation of hydration and formation of structure in hardening cement-based materials." Ph.D. thesis, Faculty of Civil Engineering and Geosciences, Dept. of Structural Engineering, Delft Univ. of Technology.

Wang, L., and T. Ueda. 2011. "Mesoscale modeling of water penetration into concrete by capillary absorption." *Ocean Eng.* 38 (4): 519–528. https://doi.org/10.1016/j.oceaneng.2010.12.019.

Ye, G. 2003. "Experimental study and numerical simulation of the development of the microstructure and permeability of cementitious materials." Ph.D. thesis, Faculty of Civil Engineering and Geosciences, Dept. of Structural Engineering, Delft Univ. of Technology.

Ye, G. 2005. "Percolation of capillary pores in hardening cement pastes." *Cem. Concr. Res.* 35 (1): 167–176. https://doi.org/10.1016/j.cemconres.2004.07.033.

Yip, M., J. Mohle, and J. Bolander. 2005. "Automated modeling of three-dimensional structural components using irregular lattices." *Comput.-Aided Civ. Inf.* 20 (6): 393–407. https://doi.org/10.1111/j.1467-8667.2005.00407.x.

Yu, S., and C. Page. 1991. "Diffusion in cementitious materials: 1. Comparative study of chloride and oxygen diffusion in hydrated cement pastes." *Cem. Concr. Res.* 21 (4): 581–588. https://doi.org/10.1016/0008-8846(91)90109-U.

Zehtab, B., and A. Tarighat. 2018. "Molecular dynamics simulation to assess the effect of temperature on diffusion coefficients of different ions and water molecules in CSH." *Mech. Time-Depend. Mater* 22 (4): 483–497. https://doi.org/10.1007/s11043-017-9368-6.

Zhang, H., B. Šavija, S. Chaves Figueiredo, M. Lukovic, and E. Schlangen. 2016. "Microscale testing and modelling of cement paste as basis for multi-scale modelling." *Materials* 9 (11): 907. https://doi.org/10.3390/ma9110907.

Zhang, H., B. Šavija, S. C. Figueiredo, and E. Schlangen. 2017. "Experimentally validated multi-scale modelling scheme of deformation and fracture of cement paste." *Cem. Concr. Res.* 102: 175–186. https://doi.org/10.1016/j.cemconres.2017.09.011.

Zhang, H., B. Šavija, M. Luković, and E. Schlangen. 2019. "Experimentally informed micromechanical modelling of cement paste: An approach coupling X-ray computed tomography and statistical nanoindentation." *Compos. Part B: Eng.* 157: 109–122. https://doi.org/10.1016/j.compositesb.2018.08.102.

Zhang, M., and A. P. Jivkov. 2016. "Micromechanical modelling of deformation and fracture of hydrating cement paste using X-ray computed tomography characterisation." *Compos. Part B-Eng.* 88: 64–72. https://doi.org/10.1016/j.compositesb.2015.11.007.